Medicinal chemistry

In Silico Design and Optimisation of Phytoalexin Resveratrol Polyphenolic Analogs as Inhibitors of Histone Acetyltransferase for the Management of Tumor Growth

Rebecca Hammett* and Dr. Clarie Shoemake

Department of Pharmacy, University of Malta, Malta

Abstract

Cancer cells are known to be more susceptible to deoxyribonucleic acid (DNA) damage than normal ones due to their genetic instability. The post-translation modification of histones plays a crucial role in chromatin regulation, influencing gene expression, DNA replication and repair. Histone acetyl transferases (HAT) are enzymes that acetylate histones, often resulting in increased gene expression and cellular proliferation. Consequently, modulators of HAT have the potential to be promising chemotherapeutic agents, due to their ability to restrict neoplastic cellular proliferation and DNA repair.

Literature suggests that resveratrol's anti-cancerous effects are a result of its inhibition of histone deacetylases, however, despite the promising efficacy of the anti-proliferative effects documented in both *in vitro* and *in vivo* studies, the precise mechanism of action of resveratrol's capability to suppress tumor growth is still under investigation. This study has consequently considered resveratrol from a different perspective, and has used this seemingly applicable molecule as a potential ligand for the p300-HAT enzyme and thus, has investigated its potential to modulate the p300-HAT ligand binding pocket (p300-HAT_LBP), a protein which is implicated in the epigenetic evolution of many epithelial and haematological malignancies. Superior novel inhibitors were designed through a dual-methodology, comprising of *de novo* and virtual screening drug design approaches.

Two structures, identified through virtual screening, specifically, Chembridge_5190757 and IBS-STOCK1N-57915, and one *de novo* generated structure, Result_133, that satisfied all measured parameters of Lipinski rule compliance, high ligand binding affinity and predicted safety upon oral administration, were identified for optimisation and *in vitro* validation, on the premise that they hold promise as clinically useful anti-neoplastic agents.

Keywords: Resveratrol; p300 Histone acetyl transferases; Protomol generation; *In silico* drug design; Anti-neoplastic agent; Acetonyl-CoA; *De novo* drug design; Virtual screening

Introduction

One of the most abundant post-translation modifications in proteins is acetylation, specifically, the most studied being *N*-ε-lysine acetylation. Acetylation enables the accessibility of transcription access to DNA by causing the neutralisation of the positively charged lysine residues or by relaxing chromatin and increasing the accessibility of transcription machinery. This implies that histone acetylation in chromatin rich regions is proportional to the level of gene expression. This balance of acetylation, and consequently gene expression, is mediated by two enzymes, HATs and histone deacetylases (HDACs) [1].

HATs are responsible for the hyperacetylation of histones, and other non-histone proteins. They act as catalysts for the acetyl-coenzmye A(CoA) dependent acetylation of the ε-amino groups of lysine residues in histones at double strand break sites, as well as in transcription co- activators and co-repressors such as E2F, p53 and GATA [2]. Besides the neutralisation of the positively charged lysines, this process also often results in transcriptional activation. On the other hand, HDAC activity induces histone hypoacetylation, in a process that releases an acetate molecule. The deacetylated lysine residues present within the histone tail give rise to an increase in the ionic interactions between the histones and DNA, which further produces an even tighter chromatin structure which limits the accessibility of the transcriptional machinery and thus facilitates gene silencing [3]. As a result, HATs and HDACs are responsible for the regulation of a variety of cellular pathways, including cellular proliferation, differentiation, apoptosis and DNA repair.

Neoplastic cells arise due to mutations resulting in altered acetylation patterns, and thus an imbalance between acetylation and deacetylation. The three principal circumstances from which altered acetylation profiles can arise include: An aberrant recruitment of HDACs on the wrong target genes, Suppressed activity of HATs, resulting in the silencing of target genes, Enhanced HAT activity at the wrong loci (example: oncogenes) due to overexpression. The above scenarios result in the alteration of the normal cellular cycle and impairment of the processes involved in cellular proliferation, differentiation and apoptosis. Depending on the site at which it occurs, both hypoacetylation and hyperacetylation influence tumorigenic proliferation [4].

Resveratrol (3,5,4'-trihydroxy-*trans*-stilbene) is a naturally occurring phytoalexin which is produced by several plants in response to injury or pathogenic attack by bacteria or fungi. Food sources of resveratrol include the skin of grapes, blueberries, raspberries, peanuts and mulberries. It exists as *cis*- and *trans*- isomers, with *trans*-

*Corresponding author: Rebecca Hammett, Department of Pharmacy, University of Malta, Msida, MSD 2080, Malta, Tel: 35623402340 E-mail: rebecca.hammett.13@um.edu.mt

resveratrol being the most dominant form, appears to be non-toxic and has greater documented anti-neoplastic and cardioprotective benefits than its corresponding *cis-* isomer [5]. For this reason, *t*-RES was chosen for modelling purposes in this study (Figure 1).

Resveratrol exhibits a broad pharmacological behavior interfering at all the three principle stages of carcinogenesis: the initiation, promotion and propagation of the cancer. Numerous studies have been carried out to investigate the anti-cancer effects of resveratrol. Amongst the proposed mechanisms of action of its anti-neoplastic effects are its affinity for p53 [7], a tumor suppressor gene, and inhibition at the HDAC active site [8]. Although the available literature suggests a variety of pathways which may contribute to its anti-neoplastic activity, malignant cells exhibit changes in multiple signaling pathways, therefore making it difficult to pinpoint the exact process which is responsible for tumor suppression.

This study has therefore considered resveratrol from a different perspective, and investigates its potential to modulate the p300-histone acetyl transferase ligand binding pocket (p300- HAT_LBP) which is implicated in multiple cancers, especially those of haematological or epithelial origin.

Materials and Methods

X-ray crystallographic deposition 4PZT [9] describing the *holo*-p300 LBP bound to an antagonist, acetonyl-CoA, was selected as a template from the Protein Data Bank. Molecular visualisation and modelling was performed in SYBYL-X v.1.2 [10]. Water molecules at a distance ≥ 5 Å from the p300-HAT_LBP were computationally eliminated, as were the small molecules, S-(1-oxopropyl)-coenzyme A and dimethylsulfoxide, owing to the fact that these were considered not relevant in the context of a static study.

The LBA of acetonyl-CoA within the LBP of its cognate receptor, p300-HAT, was determined using X-score [11]. This was calculated and expressed as the equilibrium dissociated constant (pKD). High and low affinity molecules express large and small numerical pKD values respectively. The LBA (pKD) of acetonyl-CoA was established as the baseline affinity to which all other resveratrol conformers were compared, with the intent that such conformers would have a higher LBA (pKD) than the baseline as this would imply superior binding propensity.

The 3-D structure of resveratrol was identified, and extracted from PDB crystallographic deposition 4DPN [12] describing the bound co-ordinates of resveratrol within the Conconvalin-A binding site. It was subsequently computationally docked into the HAT_LBP and conformational analysis performed. This process allowed single bond rotations of resveratrol within the p300-HAT_LBP, such that 20 optimally binding conformers of resveratrol within the p300-HAT_ LBP, with molecular displacement of 0.05 Å RMSD, were identified.

A graph of ligand binding affinity (LBA; pKD) and ligand binding energy (LBE; kcal mol^{-1}) against conformer number was plotted. The optimal resveratrol conformer was selected on the basis of combined high LBA (pKD) and low LBE (kcal mol^{-1}) on the premise that this would combine high affinity with molecular stability. This conformer was further utilised as a template for this study.

The pharmacophoric features of acetonyl-CoA when bound to its cognate receptor; p300-HAT was carried out using LigandScout v.4 [13]. Specifically, the common chemical features required for acetonyl-CoA to dock efficiently into the binding pocket of the p300-HAT enzyme, were resolved. The carrying out of such analysis was essential to this study, because, based upon the principle of molecular similarity, a molecule comprising of pharmacophoric features similar to the known inhibitor ligand, acetonyl-CoA, may be predicted to bind and produce biological effects similar to that of the template molecule. These pharmacophoric features were consequently established as baseline chemical features required for binding, and possible inhibition, of the p300-HAT_LBP.

Prior to initiation of the *de novo* phase of the study, 2-D topology maps showing the critical interactions of resveratrol within the p300-HAT_LBP were generated in PoseView [14] and BIOVIA Discovery Studio® Visualizer v.4.5 [15]. These allowed elucidation of the critical stabilising contacts forged between resveratrol and the amino acids lining the p300-HAT_LBP. Upon analysis of the 2-D topology maps it was sought to preserve at least one aromatic ring which would be able to forge the same hydrophobic interactions with Lys[1456] and a pi-cation non-covalent interaction with Arg[1462], as observed with the small molecule inhibitor, acetonyl-CoA, within the p300- HAT_LBP (Figure 2). The stilbenic double bond was also retained, on the premise that this would rigidify what was perceived to be the bioactive conformation of resveratrol, resulting in a decrease in the loss of conformational rotational entropy and thus high affinity binding. This information
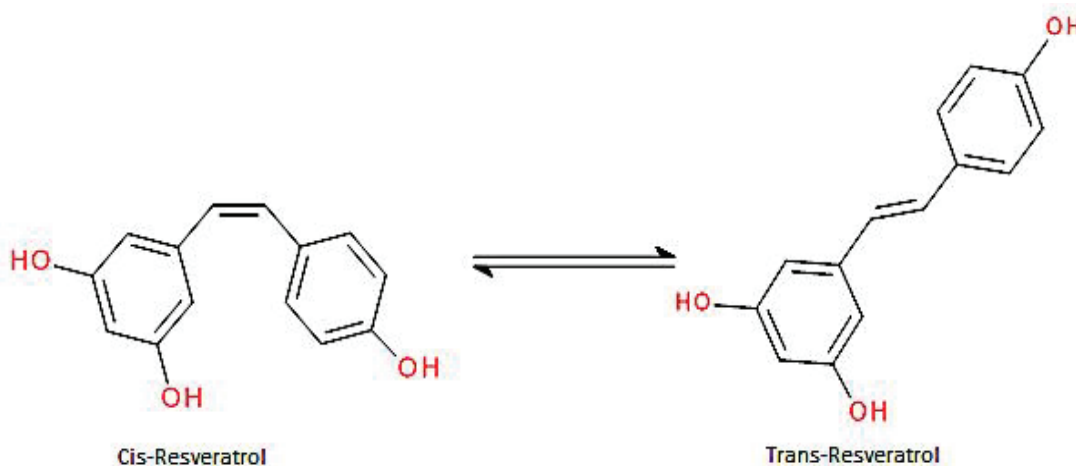

Figure 1: The chemical structures of the *cis*- and *trans*- isomers of Resveratrol rendered in BIOVIA Draw 2016 [6].
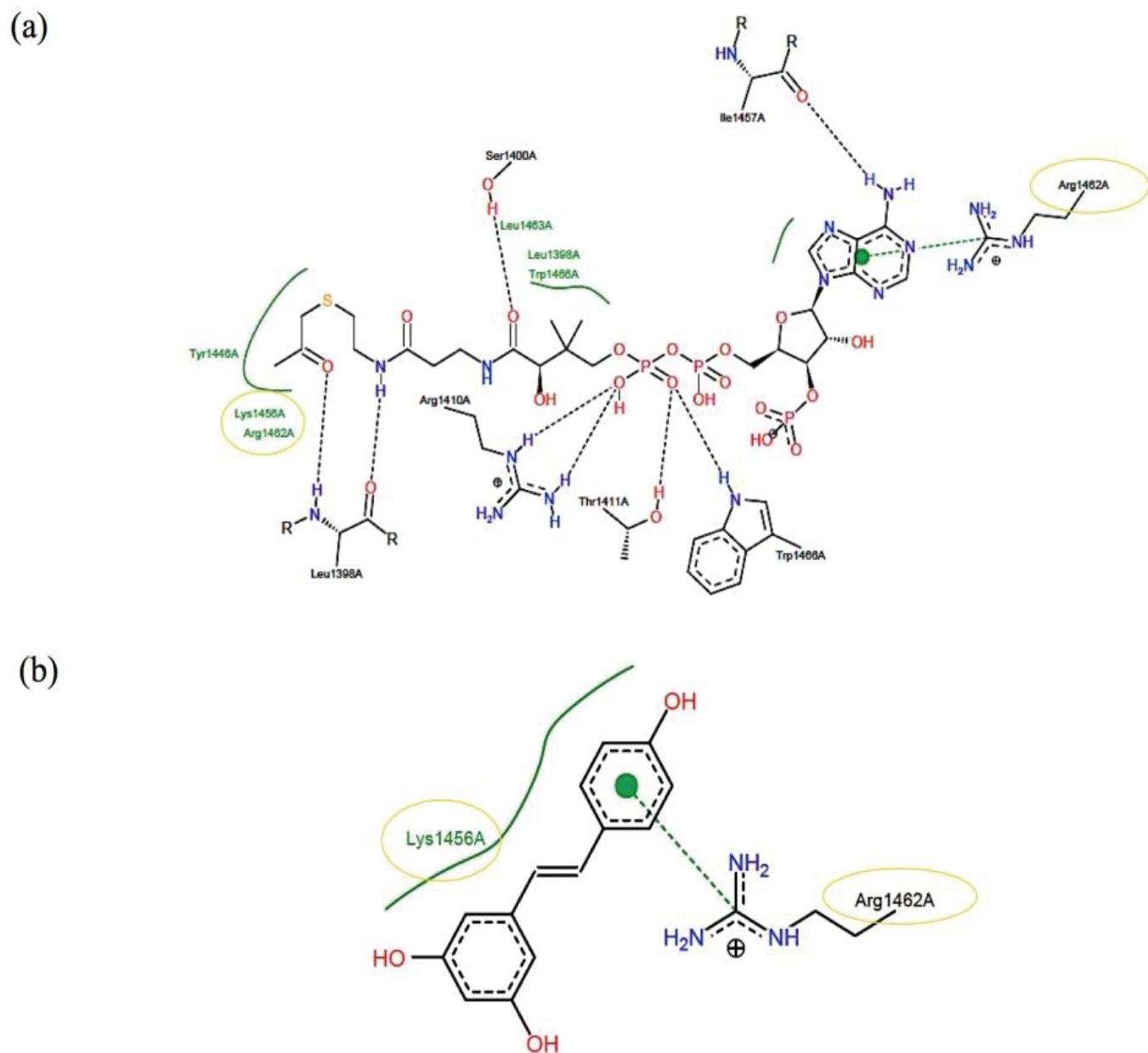
Figure 2: 2-D diagrams of the p300-HAT domain in complex with (a) Acetonyl-CoA and (b) Res_019 rendered in PoseView [14]. The 2-D depiction shows hydrogen bonds as dashed lines between the interaction partners on either side. Hydrophobic interactions are illustrated as smooth contour lines between the respective amino acids and the ligand. Similar interactions forged between the 2 ligands and amino acids within the p300-HAT domain are encircled in yellow.

consequently guided seed fragment modeling, with seed fragments being defined as high efficiency moieties capable of sustaining molecular growth within the p300-HAT_LBP.

Seed structures n=14 (Figure 3) (seeds 1-7, 14-20) were consequently modeled, which maintained to different extents, the critical moieties of resveratrol. Growing sites (H. *spc*) were assigned to the fragments such that user directed growth within the p300-HAT_LBP could be sustained.

The modeled seed fragments were based on the optimal conformation of resveratrol planted within a 3D map of the p300-HAT_LBP which was generated using the POCKET algorithm of Ligbuilder v.2 [17]. This LBP was defined according to polarity, and

proposed the pharmacophoric space within which user directed growth of the modeled seed structures could be sustained. The molecules consequently designed *de novo* were filtered to include exclusively Lipinski Rule compliant structures [18] and a LBA (pKD) that exceeded the 6.82 cut off which was the calculated LBA (pKD) of acetonyl-CoA for the p300-HAT_LBP. Molecules with a low log P were considered advantageous owing to the fact that drug delivery across the blood brain barrier was not considered necessary since the p300-HAT enzyme, the target for resveratrol considered in this study, is known to mediate primarily haematological and epithelial neoplastic conditions.

In the virtual screening approach, the optimal conformation of resveratrol, Res_019 (Figure 4), was submitted as a query to the online virtual screening applications, ViCi [19] and ZINC 12 [20]. The
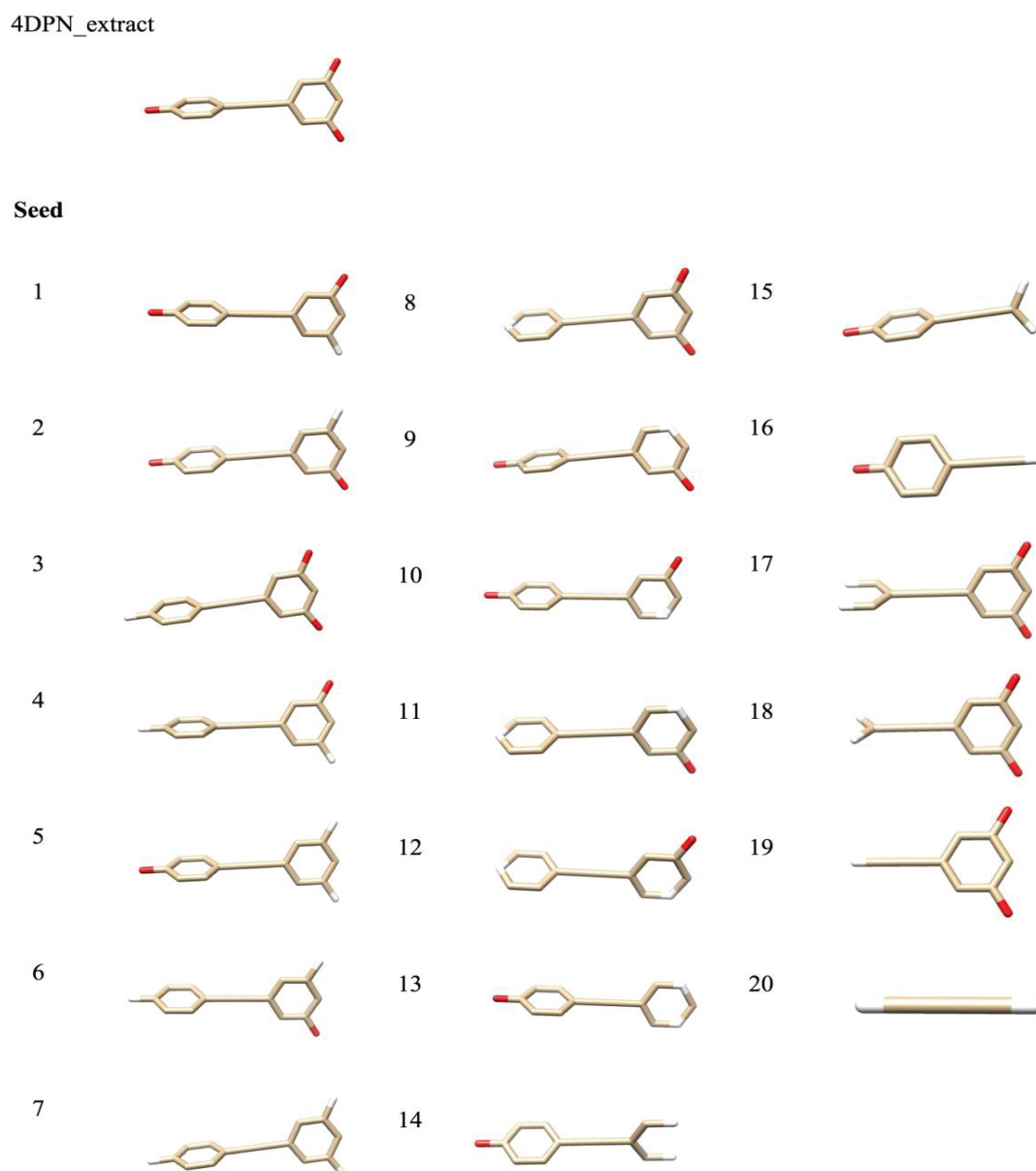
Figure 3: The 3-D structures of the Seed Structures generated in contrast to the original resveratrol molecule (4DPN_extract), rendered in UCSF Chimera [16]. Red and white tips indicate hydroxyl functional groups and *H.spc* atoms respectively.

software generated 'hit' molecules based on mathematical descriptors of molecular size, shape and electrostatic composition of the inputted ligand that would therefore also be possible ligands for the same protein (p300-HAT). The generated 'hit' molecules were filtered for Lipinski Rule compliance using Mona v.2.2 [21].

This Lipinski Rule compliant cohort of hit structures was subsequently docked into a "protomol" which was modeled in SYBYL-X v.1.2 [10]. A protomol is an idealised ligand binding pocket representing the energetically unsatisfied amino acids at the core of the target receptor. The protomol was constructed over a larger area than that that was previously accessed by the bound ligand, acetonyl-CoA, thus possibly creating a larger volume for ligand binding. The hit molecules were ranked in order of affinity to the modeled protomol.

The optimal structures identified through both the *de novo* and virtual screening approaches, were read into the online webserver

ProTox [22] for prediction of oral toxicity in rodents via estimation of their binding affinity to toxicity targets and their LD_{50} values. This was considered a crucial part of the study, owing to the fact that even if a molecule comprises of all the desired attributes of a lead molecule, it is considered useless if it is toxic upon consumption.

Results

Pharmacophoric resolution of the acetonyl-CoA moieties critical to its stabilisation within the p300-HAT_LBP showed that the most notable pharmacophoric features included two hydrophobic regions, two hydrogen bond donor centroids, nineteen hydrogen bond accepting regions and two negative ionisable areas (Figure 5). These chemical features served as a baseline for optimisation of structural chemical moieties of the selected molecules for superior ligand binding.
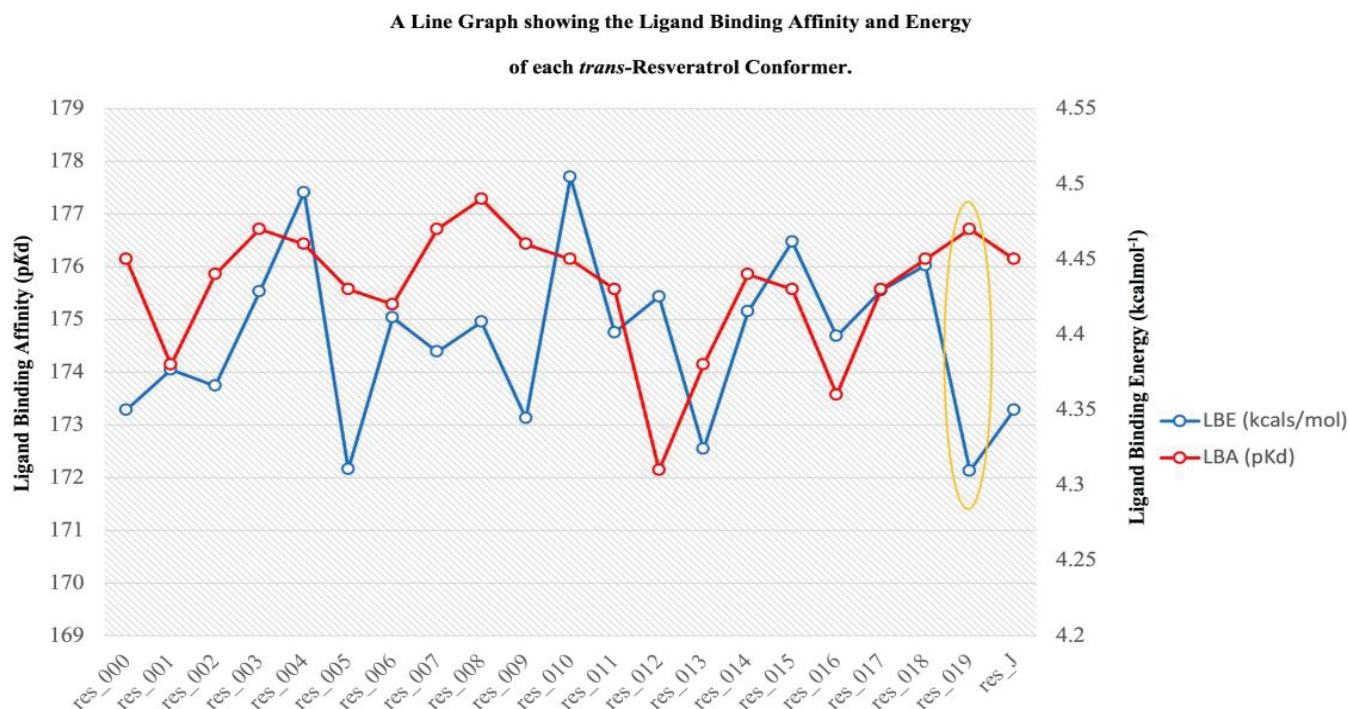
Figure 4: A line graph showing the LBE (kcal mol^{-1}) and LBA (pKD) of each conformer generated using SYBYL-X v.1.2 [10] and X-score v.1.2 [11]. The optimal binding conformer, Res_019, is encircled in yellow.
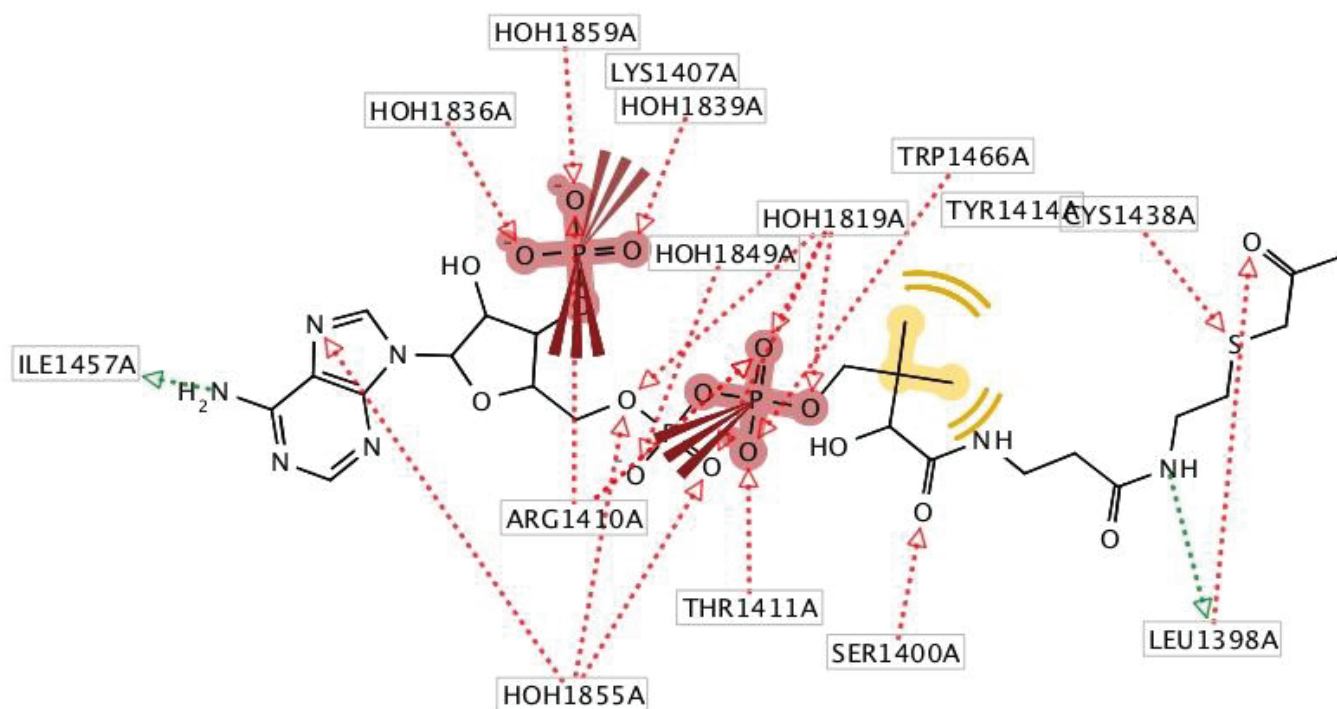

Figure 5: The pharmacophoric features of acetonyl-CoA when in complex with its cognate receptor, p300-HAT. Hydrogen bond donors are depicted in green, hydrogen bond acceptors in red, negative ionisable areas as 3 solid arrows and hydrophobic regions in yellow.

The 14 modeled seed fragments yielded a total of 558 molecules which were Lipinski Rule compliant and comprised of a superior LBA (pKD) to that of acetonyl-CoA (pKD:6.82). These were segregated into pharmacophorically similar families, and ranked, with each family according to LBA (pKD). The 10 molecules considered optimal on the basis of adherence to the inclusion criteria previously outlined above (high LBA and low logP) were identified. 1000 and 519 hits were generated using the ViCi [19] and ZINC 12 [20] virtual screening

softwares respectively, out of which 501 (50.1%) and 329 (63.39%) were Lipinski rule compliant. The 10 optimal ligands of each molecular cohort generated were identified based on their scoring function (Total_Score) (Table 1).

ProTox [22] classified the molecular cohorts from both the de novo and virtual screening processes, into different toxic classes based upon their predicted oral toxicity in rodents. This included:

Class I: Fatal if swallowed ($LD_{50} \leq 5$ mg/kg),

Class II: Fatal if swallowed ($5 < LD_{50} \leq 50$ mg/kg),

Class III: Toxic if swallowed ($50 < LD_{50} \leq 300$ mg/kg),

Class IV: Harmful if swallowed ($300 < LD_{50} \leq 2000$ mg/kg),

Class V: May be harmful if swallowed ($2000 < LD_{50} \leq 5000$ mg/kg),

Class VI: Non-toxic ($LD_{50} > 5000$ mg/kg).

Upon analysis of the distribution of the molecules amongst the different toxic classes, it was noted that *de novo* designed ligands were most likely to be harmful if swallowed (prediction accuracy approximately 54.26%). ZINC 12 [20] generated molecules were equally distributed amongst toxic classes 4 and 5 (prediction accuracy: 68.67%), while ViCi [19] generated structures were scattered amongst all classification groups (prediction accuracy ranging between 67.38% and 100%).

The molecules Chembridge_5190757 and IBS-STOCK1N-57915, identified as hits using the ViCi [19] database were regarded as the most promising ligands to be chosen for further studies owing to the fact that they were Lipinski rule compliant, had a high total-score (implying high affinity to the protomol) and that they were classified in a toxic class of 6 (non-toxic if swallowed). For comparisons sake, as well as due to the fact that the results of oral toxicities produced were against a prediction accuracy that was less than 100%, a molecule generated through the *de novo* approach, namely Result_133, that was classified in an inferior toxic class of 5 (may be harmful if swallowed), was also chosen for further analysis. The properties and 3-D structures of the chosen molecules were tabulated for ease of comparison.

Discussion

Analysis of the 2-D and 3-D structures of the virtual screening generated structures, IBS_STOCK1N-57915 and Chembridge_5190757 showed a number of similarities and differences between the two, as well as with the original lead molecule, resveratrol (Figures 6 and 7). The most remarkable difference in comparison to the original resveratrol chemical structure is that both structures did not consist of either an aromatic ring or the stilbenic double bond, which were sought to be preserved as explained above.

The two structures both comprised of a 10-membered hydrocarbon chain (decane). This might act as the hydrophobic centroid, similar to that found in the pharmacophoric structure of acetonyl_CoA (Figure 5). Whilst Chembridge_5190757 consisted of two terminal carboxylic acid groups, IBS_STOCK1N-57915 comprised of a terminal ester functional group (RCOOR'). Carboxylic acid groups may act as both a hydrogen bond acceptor and donor, whilst ester functional groups
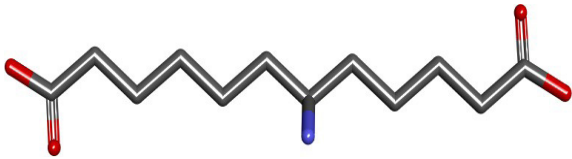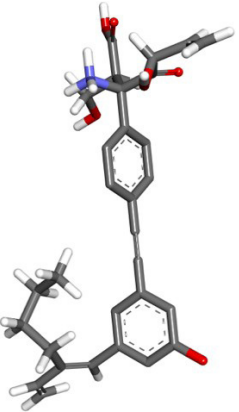
Molecule	Total_Score	LogP	HBA	HBD	MW	Toxicity Class
IBS_STOCK1N-57915 $C_{11}H_{22}NO_4$	6.64	1.62	5	3	247.33	6
Chembridge_5190757 $C_{12}H_{23}NO_4$	7.6	1.99	5	4	245.32	6
Result_133 $C_{30}H_{26}NO_6$	9.93	3.65	6	5	496	5

Table 1: Table illustrating the optimal ligands chosen for further analysis, rendered in BIOVIA Discovery Studio Visualizer v.4.5 [14]. Hydroxyl groups and amino groups are depicted in red and blue respectively.
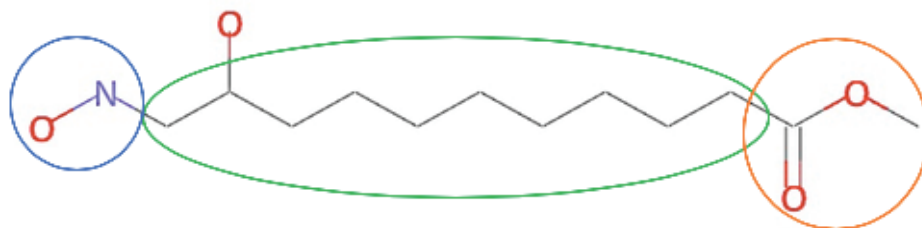
Figure 6: The 2-D structure of IBS_STOCK1N-57915 rendered in BIOVIA Discovery Studio Visualizer v.4.5 [15]. The following functional groups are encircled accordingly: decane: green, ester: orange, 2° amine: blue.
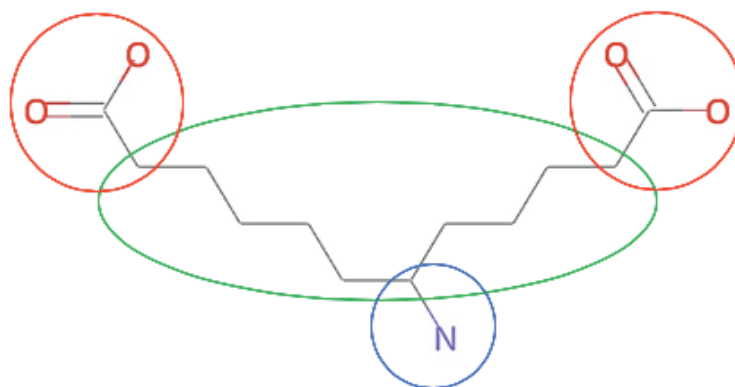

Figure 7: The 2-D structure of Chembridge_5190757 rendered in BIOVIA Discovery Studio Visualizer v.4.5 [15]. The following functional groups are encircled accordingly: decane: green, carboxylic acid: red, 1° amine: blue.

mainly act as hydrogen bond acceptors. Another notable difference is that Chembridge_5190757 has a primary amine group at C6, whilst IBS_STOCK1N-57915 consists of a secondary amine group, attached to a hydroxyl functional group and an additional hydroxyl function attached to the β-carbon of the secondary amine. Primary and secondary amines have the ability to act as both hydrogen bond donor and accepting groups.

Result_133 was a molecule constructed from the de novo drug design method. Assessment of its 2-D structure showed that it is not substantially different from the initial seed structure. From analysis of the 2-D topology maps generated using BIOVIA Discovery Studio® Visualizer v.4.5 [15] it was inferred that three of the hydroxyl functional groups (encircled in red as 1,2,3 below) and an amino group (encircled in blue), formed unfavorable donor-donor bonds with Arg[1462], Lys[1459] and Ile[1457]. However, the same amino group formed favorable hydrogen bond interactions with Ile1457. Due to the importance of hydrogen bonding with the selectivity of the molecule, the amino acid group was not considered for replacement by other chemical moieties as this could potentially result in the loss of H-bonding and specify of the molecule to the p300-HAT_LBP. However, since the hydroxyl functional groups were only involved in the formation of unfavorable donor-donor interactions, these were sought to be replaced.

Specifically, replacement of -OH (3) functional group with a methyl group may result in the formation of more stabilising interactions with the p300 protein since it will structurally create an acetonyl moiety. Maksimoska et al. described the acetonyl group of acetonyl-CoA to overlap the lysine binding site of the p300-HAT enzyme and thus forge stabilising interactions with the protein, resulting in a 10-fold increase in activity in comparison to that of acetyl-CoA (the co-factor

molecule of p300-HAT for acetylation) [9]. Thus, the introduction of the acetonyl group in the Result_133 structure at this locus might also result in a similar effect.

The replacement of the –OH (1) and (2) functional groups with methyl groups was also proposed. This could result in the generation of another hydrophobic centroid, which would make the pharmacophore of Result_133 more similar to that of acetonyl-CoA. As explained previously, acetonyl-CoA pharmacophore consisted of two hydrogen bond donors, one acceptor and two hydrophobic centres. The left hand side terminal end (Figure 8; encircled in yellow, 1) of result_133 is already hydrophobic in nature hence contributing to one hydrophobic centre of the molecule. Therefore, such structural alterations of these hydroxyl functional groups might render the other terminal end of the molecule (Figure 8; encircled in yellow, 2) more hydrophobic, and thus produce a second hydrophobic centre. Alternatively, these could also possibly be replaced with an amino functional group, capable of forging of acting as both a hydrogen bond donating and accepting group.

From the generated molecules, it is clear that the degree of innovation of virtual screening is probably greater in comparison to the *de novo* drug design approach. This is since in the *de novo* design, the optimal conformation of the resveratrol molecule was placed into the active site, and has been forced to make the same contacts as previously with the inhibitor, acetonyl-CoA. This approach is thus one that is far more stringent, as one has chosen localised growth sites, and therefore the resultant molecules were not structurally very different to the starting molecule. Alternatively, in virtual screening, one has looked at the molecule from its 3-D shape and electrostatic composition; hence it is a more exploratory approach which could potentially result in a block buster drug.
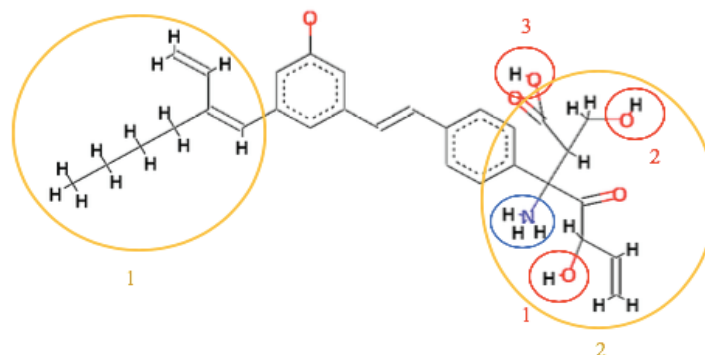
Figure 8: The 2-D structure of Result_133 rendered in BIOVIA Discovery Studio Visualizer v.4.5 [15]. The following functional groups are encircled accordingly: hydrophobic centroid: yellow, hydroxyl: red, amine: blue.

Conclusion

In conclusion, this study has used *trans*-resveratrol as a scaffold for the identification and design of high efficiency binding molecules capable of modulating the p300-HAT enzyme based upon supporting the hypothesis of high selectivity and predicted oral bioavailability. This dual approach has led to the generation of molecular cohorts whose structures and affinities may be compared, and may thus be suitable candidates for inclusion into molecular libraries that contain p300-HAT modulating properties.

This study thus proposes that this structurally diverse molecular cohort to be further explored for optimisation and *in vitro* validation, on the premise that they hold promise as clinically useful anti-neoplastic agents.

Acknowledgments

References

1. Barneda-Zahonero B, Parra M (2012) Histone deacetylases and cancer. Molecular Oncology 6: 579-589.

2. Sterner DE, Berger SL (2000) Acetylation of histones and transcription-related factors. Microbiology and Molecular Biology Reviews 64: 435-459.

3. Ropero S, Esteller M (2007) The role of histone deacetylases (HDACs) in human cancer. Molecular Oncology 1: 19-25.

4. Di Cerbo V, Schneider R (2013) Cancers with wrong HATs: the impact of acetylation. Briefings in Functional Genomics 12: 231-243.

5. Rege SD, Geeta T, Griffin GD, Broderick TL, Babu JR (2014) Neuroprotective effects of resveratrol in Alzheimer disease pathology. Frontiers in Aging Neuroscience 6: 218.

6. Biovia Draw (Computer Program) (2018) Available from: http://accelrys.com/products/collaborative-science/biovia-draw/

7. Kai L, Samuel SK, Levenson AS (2010) Resveratrol enhances p53 acetylation and apoptosis in prostate cancer by inhibiting MTA1/NuRD complex. International Journal of Cancer 126: 1538-1548.

8. Venturelli S, Berger A, Böcker A, Busch C, Weiland T, et al. (2013) Resveratrol as a pan-HDAC inhibitor alters the acetylation status of histone [corrected] proteins in human-derived hepatoblastoma cells. PLoS ONE 8: e73097.

9. Maksimoska J, Segura-Peña D, Cole PA, Marmorstein R (2014) Structure of the p300 histone acetyltransferase bound to acetyl-coenzyme A and its analogues. Biochemistry 53: 3415-3422.

10. SYBYL-X 1.2 (Computer Program) (2010) Tripos International. 1699 South Hanley Rd., St. Louis, Missouri, 63144, USA.

11. Wang R, Lai L, Wang S (2002) Further development and validation of empirical scoring functions for structure-based binding affinity prediction. Journal of Computer-Aided Molecular Design 16: 11-26.

12. Friere VN, Gottfried C, Rocha BAM, Cavada BS, Delatorre P, et al. (2013) 4DPN: Crystal structure of ConM Complexed with Resveratrol. RCSB PDB.

13. Wolber G, Langer T (2005) LigandScout: 3-D Pharmacophores Derived from Protein-Bound Ligands and Their Use as Virtual Screening Filters. Journal of Computer-Aided Molecular Design 45: 160-169.

14. Stierand K, Rarey M (2007) From modeling to medicinal chemistry: automatic generation of two-dimensional complex diagrams. Journal of Chemical Information and Modeling 2: 853-860.

15. BIOVIA Discovery Studio (2017) Dassault Systèmes BIOVIA. Discovery Studio Modeling Environment. Available from: http://accelrys.com/products/collaborative-science/biovia-discovery-studio/ Accessed on: 14 August, 2018.

16. Pettersen EF, Goddard TD, Huang CC, Couch GS, Greenblatt DM, et al. (2004) UCSF Chimera-a visualization system for exploratory research and analysis. Journal of Computational Chemistry 25: 1605-1612.

17. Yuan Y, Pei J, Lai L (2011) LigBuilder 2: A Practical de Novo Drug Design Approach. Journal of Chemical Information and Modeling 51: 1083-1091.

18. Lipinski CA (2000) Drug-like properties and the causes of poor solubility and poor permeability. Journal of Pharmacological and Toxicological Methods 44: 235-249.

19. ViCi - In-silico ligand-based drug design. EMBL. Available from: http://www.embl-hamburg.de/vici/index

20. Irwin JJ, Sterling T, Mysinger MM, Bolstad ES, Coleman RG (2012) ZINC: a free tool to discover chemistry for biology. Journal of Chemical Information and Modeling 52: 1757-1768.

21. Hilbig M, Rarey M (2015) MONA 2: A Light Cheminformatics Platform for Interactive Compound Library Processing. Journal of Chemical Information and Modeling 55: 2071-2078.

22. Drwal MN, Banerjee P, Dunkel M, Wettig MR, Preissner R (2014) ProTox: a web server for the in silico prediction of rodent oral toxicity. Nucleic Acids Research 42: 53-58.